THE JOURNAL OF PHYSICAL CHEMISTRY Letters

ACS Editors' Choice

Letter

pubs.acs.org/JPCL

Terms of Use

Electron Diffraction of Superfluid Helium Droplets

Jie Zhang, Yunteng He, William M. Freund, and Wei Kong*

Department of Chemistry, Oregon State University, Corvallis, Oregon 97331, United States

Supporting Information

ABSTRACT: We present experimental results of electron diffraction of superfluid helium droplets and droplets doped with phthalocyanine gallium chloride and discuss the possibility of performing the same experiment with a laser aligned sample. The diffraction profile of pure droplets demonstrates dependence on the nozzle temperature, that is, on the average size of the droplets. Larger clusters demonstrate faster decay with increasing momentum transfer, whereas smaller clusters converge to isolated gas phase molecules at source temperatures of 18 K and higher. Electron diffraction of doped droplets shows similar modified molecular scattering intensity as that of the corresponding gas phase molecules. On the basis of fittings of the scattering profile, the number of remaining helium atoms of the doped droplets is estimated to be on the order of hundreds. This result offers guidance in assessing the possibility of electron diffraction from laser aligned molecules doped in superfluid helium droplets.

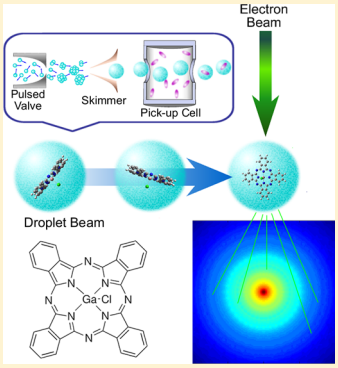

SECTION: Molecular Structure, Quantum Chemistry, and General Theory

Single molecule diffraction offers a potential solution to the problem of crystallization in crystallography.[1] By oversampling the continuous diffraction patterns from single molecules spanning all orientations (one molecule one direction at a time), sufficient information can be obtained to solve the atomic structure of the sample molecule.[2−4] However, this method relies on recording sufficient data from a single molecule—a requirement that is still difficult to fulfill even with the most recent X-ray free electron lasers. One solution to this problem is to accumulate data from multiple molecules oriented in the same direction during a series of diffraction events.[5] Additionally, different orientations need to be sampled for the necessary information on a three-dimensional structure. In this sense, single molecule diffraction needs a molecular goniometer. Different from a regular goniometer in X-ray diffraction, however, the ideal molecular goniometer should be substrate-free to avoid any interference either in the form of spurious diffraction backgrounds or in affecting the molecular conformation.

Field induced alignment or orientation offers a possible solution to the molecular goniometer. In particular, laser-induced alignment is highly desirable for charged biological macromolecules.[6−13] For effective orientation/alignment, the interaction between the induced dipole (via the polarizability anisotropy) and the fast oscillating electric field of a laser has to overcome the rotational energy of the molecule.[14] Consequently, a room temperature sample requires an impractically high field strength. Supersonic molecular beams represent a major step forward, and superfluid helium droplets with an internal temperature of 0.38 K are even more appealing.[15] The superfluidity of the droplets and the near unity relative permittivity of helium ensure minimal interference from the droplet environment to the embedded dopant. Miller's group and our own group have taken advantages of these properties and used DC electric fields for orientation and alignment of polar molecules embedded in superfluid helium droplets.[14,16] The resulting molecular alignment has been further exploited for linear dichroism spectroscopy of small biological molecules in the gas phase, such as DNA bases and amino acids.[14,17,18]

In an effort to develop a molecular goniometer for single molecule diffraction, we have recently constructed a gas phase electron diffraction (GED) apparatus[19−24] attached to a superfluid helium droplet source[25] as shown in Figure 1 (also see Supporting Information). In this work, we report our results of electron diffraction of pure superfluid helium droplets and droplets doped with phthalocyanine gallium chloride (PcGaCl). Although limited by our signal-to-noise (S/N) ratio, the resulting structure factor is not quantitative enough to derive the pair correlation function of a superfluid helium droplet; the consistent trend of our results agrees with the size variation of the droplet source. For doped droplets, the collective diffraction of helium atoms from large droplets poses a background for the dopant, and molecular diffraction is only observable with small droplets. Nevertheless, at adequate cluster sizes, features of molecular interference from PcGaCl are clearly visible.

In gas phase electron diffraction, the observed total intensity I_{total} contains contributions of all atoms of the diffractive species $I_{at}(s)$ and coherence between each unique pairs of atoms $I_{mol}(s)$, where s is the momentum transfer during diffraction[19]

$$s = \frac{4\pi}{\lambda}\sin\left(\frac{\theta_d}{2}\right) \quad (1)$$

Received: April 7, 2014
Accepted: May 7, 2014
Published: May 7, 2014

   dx.doi.org/10.1021/jz5006829 | J. Phys. Chem. Lett. 2014, 5, 1801−1805

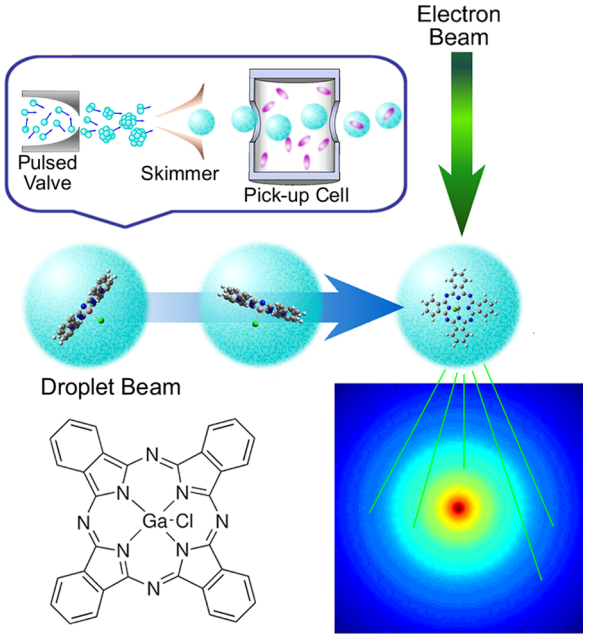

Figure 1. Experimental apparatus showing the electron beam and the PcGaCl doped superfluid helium droplet beam. The simulated diffraction pattern on a logarithmic scale and the molecular structure are also shown.

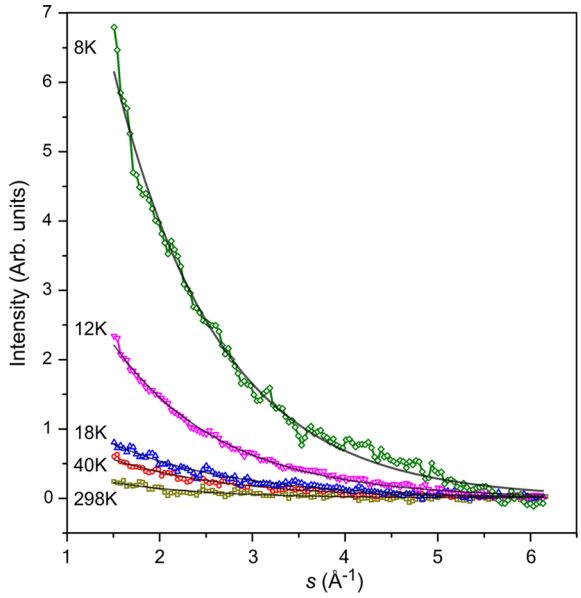

Figure 2. Total electron diffraction intensity from pure superfluid helium droplets. The smooth line shows single exponential fits to the experimental curve. The resulting width parameter, the estimated size of the droplet, and the percent of surface atoms are listed in Table 1.

λ is the de Broglie wavelength (0.06 Å at 40 keV), and θ_d is the diffraction angle. The small elastic and inelastic diffraction cross sections of each atom, typically much less than 0.01 Å^2, guarantee that there is no absorption and, hence, no heating effect from the electron beam.[26] For the same reason, secondary diffractions are also negligible even for helium droplets of submicrometer in size. A randomly oriented molecular sample produces a circularly symmetric diffraction pattern, and the structure-sensitive component is typically shown as modified molecular scattering intensity $sM(s)$

$$sM(s) = \frac{sI_{mol}}{I_{at}} = s\frac{I_{total} - I_{at}}{I_{at}} \quad (2)$$

Modeling of the modified molecular scattering intensity from GED, therefore, includes removal of the known contributions of the constituent atoms of the diffractive molecule. In our case of diffraction from molecules embedded in superfluid helium droplets, the observed intensity has additional contributions from the surrounding helium atoms of the droplet. As will be seen in the following, this complication of the droplet poses a problem for randomly oriented molecular species as in standard GED, but its effect can be removed by background subtraction for aligned or oriented species.

We have first recorded the electron diffraction pattern of pure helium droplets under different temperatures of the helium source, and the diffraction intensity I_{total} as a function of momentum transfer s is shown in Figure 2. The diffraction intensity increases with the decrease in temperature of the droplet source, and the decay rate also exhibits dependence on the source temperature. We have used a single exponential function to fit the decay of the diffraction profiles, and the resulting width parameters (w) from the fitting are listed in Table 1. Two distinct groups can be recognized from the data: those with source temperatures ≤12 K that have higher diffraction intensities and narrower distributions and those with temperatures ≥18 K that have weaker intensities and slower decays. In fact, the diffraction profiles of the latter group are essentially identical to that of pure helium gas at 298 K (included in Table 1 and Figure 2). We have then attempted a biexponential fitting for the lower temperature group (≤12 K) with one of the exponents fixed at 1.48 Å^{-1} (exponent of the higher temperature group), and the resulting second exponential function has a much faster decay, on the order of 0.3 Å^{-1}. We have also performed statistical analysis (F-test) and confirmed the biexponential nature of the decay profiles. For further evidence, we have performed a biexponential analysis for the higher temperature group and confirmed the single exponential nature of the experimental data. Other fitting functions including power law and Gaussian functions, as listed in Table 1, have also been attempted, but the quality of the fitting is visibly worse than that of the exponential functions. In all cases, however, the conclusion with regard to the two distinct groups of decay profiles remains the same.

The amplitude of the exponential fitting is affected by many factors. Under constant electron fluxes and constant gas fluxes from the nozzle, the amplitude from atomic diffraction should be similar. The amplitude from molecular diffraction, that is, coherent diffraction from a correlated atom pair, should be related to the number of helium pairs within each droplet. For the higher temperature group with negligible coherent molecular diffraction, we therefore expect similar amplitudes of atomic diffraction because the total number of atoms arriving at the diffraction region is similar. This expectation is qualitatively confirmed in Figure 2. From 12 to 8 K, on the other hand, we do expect a rise in diffraction amplitude due to the presence of correlated atom pairs in large droplets, again as evidenced from Figure 2.

Compared with previous reports of neutron diffraction of bulk superfluid helium,[27−29] our monotonic decay profiles lack the weak oscillatory portion of the pair correlation function at large s values. We attribute this difference to two reasons: one is the polydispersity in the size of the droplets and the other is the variation in density from the core to the surface of a helium

dx.doi.org/10.1021/jz5006829 | J. Phys. Chem. Lett. 2014, 5, 1801−1805

Table 1. Width Parameters (w) from Electron Diffraction Profiles of Superfluid Helium Droplets

source temperature	8 K	12 K	18 K	40 K	298 K
exponential $y = y_0 + A{\cdot}e^{(-s/w)}$	1.25 ± 0.03	1.27 ± 0.03	1.49 ± 0.11	1.48 ± 0.10	1.68 ± 0.21
allomeric $y = y_0 + A{\cdot}s^{-w}$	2.48 ± 0.05	2.42 ± 0.04	2.18 ± 0.07	2.22 ± 0.07	2.15 ± 0.12
Gaussian $y = y_0 + A{\cdot}e^{(-s^2/2w^2)}$	1.87 ± 0.02	1.91 ± 0.02	2.08 ± 0.04	2.04 ± 0.04	2.02 ± 0.05
droplet size	10^6 (220 Å)	10^5	10^3 (22 Å)	$<10^3$	1
surface atoms (%)	8	17	60	>60	100

droplet. Theoretical simulations of superfluid helium droplets have revealed a diffuse surface layer and a bulklike interior for a droplet of over 100 atoms.[30,31] Although the droplet size distribution varies from setup to setup for pulsed droplet sources, we can try to use the average droplet size from ref 32 as a general guide. If we further assume a surface layer of 6 Å, the resulting percent of surface atoms under each source temperature is listed in Table 1. Below 12 K, most of the atoms in a droplet are considered interior atoms, whereas above 18 K, diffuse surface atoms dominate. In this sense, biexponential functions should be better representations of the experimental data at the two lowest source temperatures, a point confirmed from our statistical analysis.

On the basis of Figure 2, when the source temperature is above 18 K, diffraction profiles of the droplet beam are essentially the same as that of gas phase helium atoms, consisting of only incoherent atomic scattering. The negligible pair correlation between atoms of small droplets is essential for the analysis of the diffraction pattern of doped droplets: all recorded coherent molecular scattering should be from the doped molecules, whereas coherence of the surrounding helium atoms can be neglected.

Figure 3 shows the modified molecular scattering intensity $sM(s)$ at a source temperature of 20 K after removing the

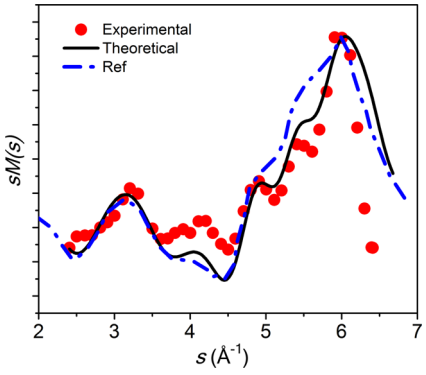

Figure 3. Modified molecular scattering intensity $sM(s)$ of PcGaCl embedded in helium droplets (dot and solid line) at a source temperature of 20 K, and the $sM(s)$ of gaseous PcGaCl from ref 33 for comparison (dot-dashed line).

contribution of incoherent atomic scattering using eq 2. The best source temperature for the highest diffraction signal has been obtained at 20 K, which is comparable to that from our laser-induced fluorescence experiment.[25] The signal-to-noise ratio is limited even after 360 000 repetitions, but the overall pattern is in agreement with our calculation and a previous report from gas phase electron diffraction.[33] Background signals, from the optical interference of the hot filament electron gun and from the ambient gas including sample molecules migrated into the diffraction region, have been recorded with equal exposure times and have been removed from the data.

We have tried three different methods of calculation to cross-check the theoretical diffraction pattern. First, standard software packages can be downloaded from the Web site of Rowland Institute at Harvard.[34] For the input file of this calculation, the geometry of the molecule has been obtained from Gaussian 09[35] (DFT/B3LYP with cc-pvtz basis set). Second, the Fourier transform of the electron density distribution obtained from the same Gaussian calculation can be used for one orientation of the molecular frame, and full rotation of the molecular frame has been achieved using a program written in Matlab. Third, we have also written our own code for treating each atom as a scattering source and have calculated the resulting interference pattern with full rotation of the molecular frame. In all cases, the same modified molecular scattering intensity has been obtained for the gas phase sample.

In calculating the theoretical diffraction profile of doped droplets, we have treated the number of helium atoms in each droplet as an adjustable parameter, and optimization has been visually performed by comparing the resulting profile with the experimental data. The effective number of helium atoms for the fitting is between 100 and 150.

Although the quality of the experimental data is still low, improvements can be readily achieved in several aspects. First, our camera has no intensification capability and has only one stage of thermoelectric cooling, and a glass window (for vacuum seal) between the phosphor screen and the camera has limited transmission. Upgrade of the image detection system will improve the S/N by perhaps several folds. Second, although the electron gun has the potential of offering a much higher flux (an extra order of magnitude), we have been unable to fully utilize this feature because of two practical issues: one has been the optical contamination on the camera due to the hot-filament of the electron gun and the other has been the need for another magnetic lens necessary to obtain a collimated small beam for diffraction. Improvement in the electron beam has the potential of further increasing S/N by an order of magnitude.

A major motivation of the current experiment is to assess the feasibility of using superfluid helium as a cooling agent for laser-induced alignment of embedded biological molecules in diffraction experiments. The degree of alignment/orientation is a major factor in determining the ultimate resolution of the resulting structure.[36] The extreme temperature of superfluid helium droplets can lower the necessary field strength by nearly 4 orders of magnitude for a biological molecule coming from a room temperature vaporization source. Consequently, only moderate fields are necessary for the often fragile sample, a condition much more preferred than otherwise. However, superfluid helium surrounding an embedded molecule generates a diffraction background. Fortunately, this background can be effectively removed for aligned or oriented samples. Randomly oriented samples and all atoms in the sample

dx.doi.org/10.1021/jz5006829 | J. Phys. Chem. Lett. 2014, 5, 1801−1805

contribute to an isotropic diffraction pattern. In contrast, the structurally informative molecular diffraction from spatially aligned or oriented molecules is anisotropic. Consequently, all isotropic contributions, including those from helium atoms and those from all atoms of the molecular sample, can be removed by a direct subtraction between diffraction patterns with and without sample alignment/orientation. This subtraction can remove the uncertainty in the number of helium atoms of each droplet and any residual coherence between helium atoms in the interior structure of a large droplet. In this sense, diffraction from aligned samples has the advantage of removing the polydispersity of the droplet beam. However, because this process takes the difference of two large signals, the key is not to overwhelm the detector with the intense diffraction of helium atoms surrounding the sample molecule. At 40 keV, the relative atomic diffraction cross section of helium and carbon is 3:40;[37] hence, it takes ∼10 helium atoms to be competitive with a carbon atom. In the current experiment, the ratio of carbon to helium atoms is about 1:5. Improvement in the detector should be able to increase the tolerance of the helium to carbon ratio to a much higher level.

In conclusion, we have demonstrated electron diffraction of pure superfluid helium droplets and doped droplets with a neutral molecule. The diffraction profile of pure helium droplets is affected by the polydispersity of the droplet beam, but it is in qualitative agreement with the size variation of the droplets. Larger droplets with a substantial compact interior component demonstrate stronger diffraction and faster decay with momentum transfer, whereas smaller droplets converge to gas phase isolated molecules when the droplet source temperature reaches 18 K. Electron diffraction of PcGaCl doped in helium droplets is possible with small droplets. Although the surrounding helium atoms contribute to the background of the experiment, this interference can be removed in diffraction from an aligned or oriented sample. As long as the detector is not overwhelmed by the isotropic background of the helium atoms, diffraction of aligned samples is possible and advantageous over that of randomly oriented samples.

■ ASSOCIATED CONTENT

Supporting Information

Information on details of the experimental setup, including the superfluid helium droplet source, the electron beam, and the imaging system is provided in the supplemental document. In addition, a raw image and the diffraction profile from averages of raw images are also included. The atomic contribution is overlaid with the diffraction profile for comparison. This material is available free of charge via the Internet at http://pubs.acs.org/.

■ AUTHOR INFORMATION

Corresponding Author

*E-mail: wei.kong@oregonstate.edu. Phone: 541-737-6714. Fax: 541-737-2062.

Notes

The authors declare no competing financial interest.

■ ACKNOWLEDGMENTS

This work is supported by the National Institute of General Medical Sciences (1RC1GM092054-01) from the National Institutes of Health. The content is solely the responsibility of the authors and does not necessarily represent the official views of the National Institutes of Health. Additional support from the National Science Foundation (CHE-0827182), the Murdock Charitable Trust, the Oregon Nanoscience and Microtechnologies Institute, and the Environmental Health Science Center at Oregon State University funded by the National Institute of Environmental Health Sciences (ES000240) are also deeply appreciated. Special thanks are to Dr. Toennies for his continued encouragement of this project. We also thank our collaborator Dr. Joe Beckman for his unwavering support over the past few years.

■ REFERENCES

(1) Neutze, R.; Wouts, R.; van, d. S. D.; Weckert, E.; Hajdu, J. Potential for Biomolecular Imaging with Femtosecond X-ray Pulses. *Nature* **2000**, *406*, 752−757.

(2) Fienup, J. R. Phase Retrieval Algorithms: A Comparison. *Appl. Opt.* **1982**, *21*, 2758−2769.

(3) Miao, J.; Charalambous, P.; Kirz, J.; Sayre, D. Extending the Methodology of X-ray Crystallography to Allow Imaging of Micrometre-Sized Non-Crystalline Specimens. *Nature (London)* **1999**, *400*, 342−344.

(4) Capotondi, F.; Pedersoli, E.; Mahne, N.; Menk, R. H.; Passos, G.; Raimondi, L.; Svetina, C.; Sandrin, G.; Zangrando, M.; Kiskinova, M.; et al. Invited Article: Coherent Imaging Using Seeded Free-Electron Laser Pulses with Variable Polarization: First Results and Research Opportunities. *Rev. Sci. Instrum.* **2013**, *84*, 051301/1−051301/11.

(5) Spence, J. C. H.; Doak, R. B. Single Molecule Diffraction. *Phys. Rev. Lett.* **2004**, *92*, 198102/1−198102/4.

(6) Friedrich, B.; Herschbach, D. R. Spatial Orientation of Molecules in Strong Electric Fields and Evidence for Pendular States. *Nature* **1991**, *353*, 412−414.

(7) Normand, D.; Lompre, L. A.; Cornaggia, C. Laser-Induced Molecular Alignment Probed by a Double-Pulse Experiment. *J. Phys. B: At., Mol. Opt. Phys.* **1992**, *25*, L497−L503.

(8) Dietrich, P.; Strickland, D. T.; Laberge, M.; Corkum, P. B. Molecular Reorientation during Dissociative Multiphoton Ionization. *Phys. Rev. A: At., Mol., Opt. Phys.* **1993**, *47*, 2305−2311.

(9) Kim, W.; Felker, P. M. Spectroscopy of Pendular States in Optical-Field-Aligned Species. *J. Chem. Phys.* **1996**, *104*, 1147−1150.

(10) Kumar, G. R.; Gross, P.; Safvan, C. P.; Rajgara, F. A.; Mathur, D. Molecular Pendular States in Intense Laser Fields. *J. Phys. B: At., Mol. Opt. Phys.* **1996**, *53*, 3098−3102.

(11) Larsen, J. J.; Hald, K.; Bjerre, N.; Stapelfeldt, H.; Seideman, T. Three Dimensional Alignment of Molecules Using Elliptically Polarized Laser Fields. *Phys. Rev. Lett.* **2000**, *85*, 2470−2473.

(12) De, S.; Znakovskaya, I.; Ray, D.; Anis, F.; Johnson, N. G.; Bocharova, I. A.; Magrakvelidze, M.; Esry, B. D.; Cocke, C. L.; Litvinyuk, I. V.; et al. Field-Free Orientation of CO Molecules by Femtosecond Two-Color Laser Fields. *Phys. Rev. Lett.* **2009**, *103*, 153002/1−153002/4.

(13) Oda, K.; Hita, M.; Minemoto, S.; Sakai, H. All-Optical Molecular Orientation. *Phys. Rev. Lett.* **2010**, *104*, 213901/1−213901/4.

(14) Kong, W.; Pei, L.; Zhang, J. Linear Dichroism Spectroscopy of Gas Phase Biological Molecules Embedded in Superfluid Helium Droplets. *Int. Rev. Phys. Chem.* **2009**, *28*, 33−52.

(15) Toennies, J. P.; Vilesov, A. F.; Whaley, K. B. Superfluid Helium Droplets: An Ultracold Nanolaboratory. *Phys. Today* **2001**, *54*, 31−37.

(16) Dong, F.; Miller, R. E. Vibrational Transition Moment Angles in Isolated Biomolecules: A Structural Tool. *Science (Washington, DC, U. S.)* **2002**, *298*, 1227−1230.

(17) Choi, M. Y.; Miller, R. E. Infrared Laser Spectroscopy of Imidazole Complexes in Helium Nanodroplets: Monomer, Dimer, and Binary Water Complexes. *J. Phys. Chem. A* **2006**, *110*, 9344−9351.

(18) Choi, M. Y.; Miller, R. E. Four Tautomers of Isolated Guanine from Infrared Laser Spectroscopy in Helium Nanodroplets. *J. Am. Chem. Soc.* **2006**, *128*, 7320−7328.

(19) Brockway, L. O. Electron Diffraction by Gas Molecules. *Rev. Mod. Phys.* **1936**, *8*, 231−266.
(20) Fink, M.; Bonham, R. A. High Precision Electron Diffraction Unit for Gases. *Rev. Sci. Instrum.* **1970**, *41*, 389−396.
(21) Torchet, G.; Farges, J.; De Feraudy, M. F.; Raoult, B. Structural Transition in Sulfur Hexafluoride Clusters. *Z. Phys. D: At., Mol. Clusters* **1989**, *12*, 93−96.
(22) Hedberg, K. Gas-Phase Electron Diffraction Applied to Molecules Undergoing Large-Amplitude Motion. *NATO ASI Ser., Ser. C* **1993**, *410*, 423−445.
(23) Rankin, D. W. H.; Robertson, H. E. Gas-Phase Molecular Structures Determined by Electron Diffraction. *Spectrosc. Prop. Inorg. Organomet. Compd.* **1995**, *28*, 428−50.
(24) Maier-Borst, M.; Cameron, D. B.; Rokni, M.; Parks, J. H. Electron Diffraction of Trapped Cluster Ions. *Phys. Rev. A: At., Mol., Opt. Phys.* **1999**, *59*, R3162−R3165.
(25) Pei, L.; Zhang, J.; Kong, W. Electronic Polarization Spectroscopy of Metal Phthalocyanine Chloride Compounds in Superfluid Helium Droplets. *J. Chem. Phys.* **2007**, *127*, 174308/1−174308/8.
(26) Bonham, R. A.; Ng, E. W. Calculation of Total Electron Inelastic Scattering Cross Sections for Neutral Atoms in the keV Energy Range. *Chem. Phys. Lett.* **1969**, *4*, 355−357.
(27) Hurst, D. G.; Henshaw, D. G. Atomic Distribution in Liquid Helium by Neutron Diffraction. *Phys. Rev.* **1955**, *100*, 994−1002.
(28) Svensson, E. C.; Sears, V. F.; Woods, A. D. B.; Martel, P. Neutron-Diffraction Study of the Static Structure Factor and Pair Correlations in Liquid Helium-4. *Phys. Rev. B: Condens. Matter* **1980**, *21*, 3638−3651.
(29) Sosnick, T. R.; Snow, W. M.; Sokol, P. E.; Silver, R. N. Momentum Distributions in Liquid Helium-4. *Europhys. Lett.* **1989**, *9*, 707−712.
(30) Cheng, E.; McMahon, M. A.; Whaley, K. B. Current and Condensate Distributions in Rotational Excited States of Quantum Liquid Clusters. *J. Chem. Phys.* **1996**, *104*, 2669−2683.
(31) Harms, J.; Toennies, J. P.; Dalfovo, F. Density of Superfluid Helium Droplets. *Phys. Rev. B: Condens. Matter Mater. Phys.* **1998**, *58*, 3341−3350.
(32) Gomez, L. F.; Loginov, E.; Sliter, R.; Vilesov, A. F. Sizes of Large He Droplets. *J. Chem. Phys.* **2011**, *135*, 154201/1−154201/9.
(33) Strenalyuk, T.; Samdal, S.; Volden, H. V. Molecular Structures of Chloro(Phthalocyaninato)-Aluminum(III) and -Gallium(III) as Determined by Gas Electron Diffraction and Quantum Chemical Calculations: Quantum Chemical Calculations on Fluoro-(Phthalocyaninato)-Aluminum(III) and -Gallium(III), Chloro-(Tetrakis(1,2,5-Thiadiazole)Porphyrazinato)-Aluminum(III) and -Gallium(III) and Comparison with Their X-ray Structures. *J. Phys. Chem. A* **2008**, *112*, 9075−9082.
(34) Cameron, D.; Parks, J. GPED Simulator. http://www.genetical.com/dc/ScientificResearch/Rowland/GPED/Usage.html.
(35) Frisch, M. J.; Trucks, G. W.; Schlegel, H. B.; Scuseria, G. E.; Robb, M. A.; Cheeseman, J. R.; Scalmani, G.; Barone, V.; Mennucci, B.; Petersson, G. A., et al. *Gaussian 09*, Revision A.1; Gaussian, Inc.: Wallingford, CT, 2009.
(36) Starodub, D.; Doak, R. B.; Schmidt, K.; Weierstall, U.; Wu, J. S.; Spence, J. C. H.; Howells, M.; Marcus, M.; Shapiro, D.; Barty, A.; et al. Damped and Thermal Motion of Laser-Aligned Hydrated Macromolecule Beams for Diffraction. *J. Chem. Phys.* **2005**, *123*, 244304/1−244304/7.
(37) Srd E-Commerce System, Nist Electron Elastic-Scattering Cross-Section Database, Version 3.2. https://www-s.nist.gov/srd_online/index.cfm?fuseaction=home.main&productID=SRD64v3.2.